SPACE TELESCOPE SCIENCE INSTITUTE
Operated for NASA by AURA

Instrument Science Report WFC3 2007-09

UVIS Channel Ghosts after Filter Replacement

Thomas M. Brown
Apr 26, 2007

ABSTRACT

The first ambient and thermal vacuum tests for WFC3 discovered significant filter ghosts due to reflections between filter substrates. Those filters with the most problematic ghosting were replaced in the instrument. The current ground test campaign, using the UVIS spare detector (UVIS build 2), includes imaging through these replacement filters to verify the mitigation of the ghosts. The results confirm that the ghosts in these filters have been significantly reduced in strength and complexity.

Background

WFC3 was designed as a general-purpose instrument, providing wide-field imaging capabilities over a large wavelength range with a versatile filter set. The WFC3 UVIS filters pushed the technological envelope to sculpt the shape of the bandpasses. An ideal filter has sharp transitions in throughput at the long and short wavelength cutoffs, and low light leak outside of the nominal bandpass. Some of the UVIS filters use metallic coatings and multiple substrates to achieve the desired bandpass, while the long-wavelength narrow-band filters employ air gaps between substrates, but these innovations can cause ghosting. During the first ambient and thermal vacuum tests of the instrument, it was discovered that some of the filters exhibited significant ghosting, with a wide range in strength, complex morphology, field dependence, and wavelength dependence (Brown & Lupie 2004, ISR WFC3 2004-04). Filter ghosts were most significant in the *F218W*, *F225W*, FQ232N, FQ243N, *F275W*, *F280N*, *F300X*, *F410M*, *F467M*, F547M, *F606W*, *F621M*, F625W, F656N, *F658N*, F665N, F673N, F680N, F689M, and F775W filters. Most of these filters were replaced (indicated in italics), often showing improved throughput in addition to ghost mitigation. Besides these filters, the F600LP was replaced with its flight spare due to a

procedural error, while the F588N was replaced with the F200LP due to concerns with the filter edge stability.

In the current ground testing campaign, we included two tests to measure ghost levels in all bandpasses that exhibited ghosts previously, whether they were intrinsic to the filter or due to reflections in the detector package. These tests were performed in the same manner as described in Brown & Lupie (2004), with the "CASTLE" optical stimulus providing a broad-spectrum point source from its Xenon lamp. A short unsaturated image was obtained to indicate the source flux, followed by a longer saturated image to characterize the ghosts. Most filters were measured at one field position with an 800x800 pixel subarray, but the F225W, F606W, and F280N filters were measured at multiple field positions with both 800x800 pixel subarrays and full-frame images binned 2x2 pixels. The analysis of the raw images was done in the same manner described in Brown & Lupie (2004), using the same IDL software, with minor modifications to account for changes in the keywords of the FITS file headers. In short, irregularly-shaped apertures were placed around each ghost, and compared to appropriate regions free of ghosts by reflecting about the position of the point source. The signal in the ghost was then compared to the signal in the point source by obtaining aperture photometry of the point source in the unsaturated exposure.

Results

The characterization of the ghosts in the current test is summarized in Table 1 and Figures 1 through 24. The "ghost strength" in the table is the signal in the ghost relative to the signal in the point source. All of the filters that were replaced show significant improvement in the ghosting levels, with the ghosts now undetectable in some cases. The measurements here agree well with the acceptance tests of Baggett et al. (2004, ISR WFC3 2007-01); in some cases their measurements implied somewhat stronger ghosts, but their test setup (using bare filters with a collimated lamp source) was primarily intended for relative ghost measurements between candidate filters. For those filters that were remeasured here but not replaced since the 2004 ground test campaign, the new measurements generally agree with the old measurements (Brown & Lupie 2004), although the proximity of the ghosts to the point source makes them difficult to measure precisely, and the dependence upon source field position somewhat hampers a direct comparison.

For the UV filters that were replaced, the ghost morphology has become a simple donut, in contrast to the very complex shapes produced by the old filters. In particular, the extreme scattering seen in the original F280N filter, due to surface deterioration and multiple filter layers, is now replaced by a simple, weaker ghost from the replacement filter. The numerous compact filter ghosts present in the original F606W and F621M filters are no longer present in the replacements. The donut-shaped filter ghosts in the F658N are clearly fainter with the new filter.

Regardless of filter replacement, many of the images still exhibit extended donut-shaped ghosts from the detector windows, especially at longer wavelengths. The window ghosts here are often somewhat fainter than they were in 2004, but there are several factors that may contribute to this: slight differences in the window coatings for this detector (UVIS build 2), differences in the lamp spectrum, and differences in the field position of the source.

Table 1: Ghost characterization

Filter	Fig.	ghost strength measured in 2007	description	ghost strength measured in 2004
F218W	1	1.3% in one	donut from filter	10% in all
F225W	2, 22	0.4% in all	donuts from filter	15% in all
F275W	3	<0.1%	-	0.7% in one
F300X	4	0.3% in one	donut from filter	1% in one
F410M	5	<0.1%	possible compact ghosts from filter	0.6% in all
F467M	6	<0.1%	possible compact ghosts from filter	0.3% in all
F547M (not replaced)	7	<0.1%	window donuts and compact filter ghosts	<0.1%
F606W	8, 24	0.4% in all	window donuts, but previous compact filter ghosts are gone	0.4% in donuts 0.3% in compact ghosts
F621M	9	0.2% in all	window donuts, but previous compact filter ghosts are gone	0.4% in donuts 0.3% in compact ghosts
F625W (not replaced)	10	0.2% in all <0.1% per ghost	window donuts and compact filter ghosts	<0.1% per ghost
F689M (not replaced)	11	0.5% in all 0.1% per compact ghost	window donuts and compact filter ghosts	0.5% in all 0.1% per compact ghost
F775W (not replaced)	12	0.3% in all <0.1% per ghost	window donuts and compact filter ghosts	<0.1% per ghost
F814W (not replaced)	13	0.3% in all	window donuts	0.4% in all

Filter	Fig.	ghost strength measured in 2007	description	ghost strength measured in 2004
FQ232N (not replaced)	14	5% in brightest 7% in all	filter donuts	4% in brightest 1% in second ghost
FQ243N (not replaced)	15	3% in brightest 5% in all	filter donuts	2% in brightest 1% in second ghost
F280N	16, 23	0.6% in one	filter donut	10-50% in ghosts and scattered light, field dependent
F656N (not replaced)	17	0.4% filter <0.1% window	donuts	0.5% filter 0.4% window
F658N	18	0.4% filter 0.1% window	donuts	0.9% filter 0.4% window
F665N (not replaced)	19	0.1% filter 0.2% window	donuts	0.4% filter 0.4% window
F673N (not replaced)	20	0.3% filter 0.1% window	donuts	0.3% filter 0.4% window
F680N (not replaced)	21	0.3% filter 0.1% window	donuts	0.3% filter 0.1% window

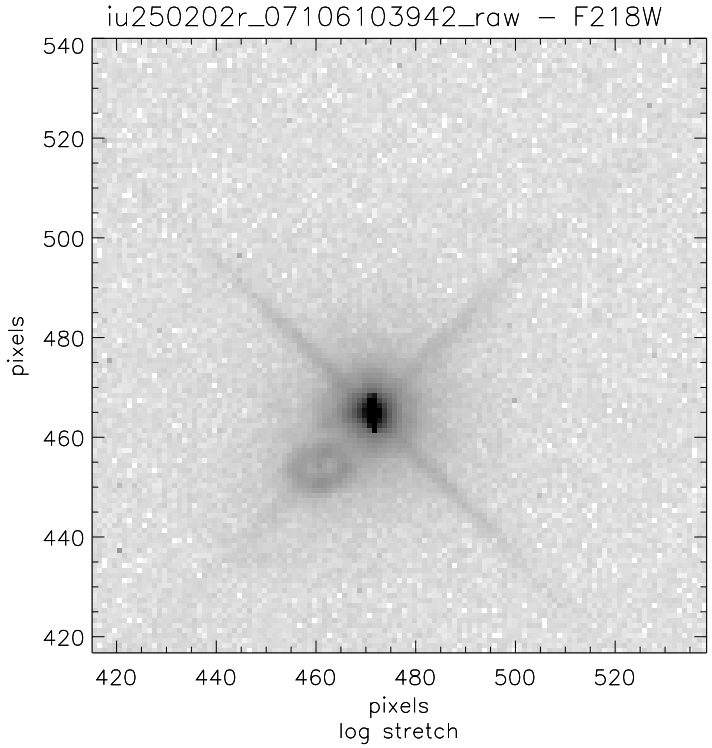

Figure 1: A saturated image with a logarithmic stretch, taken with the F218W filter. A donut ghost from the filter, at 1.3% the strength of the source, is apparent to the lower left of the source.

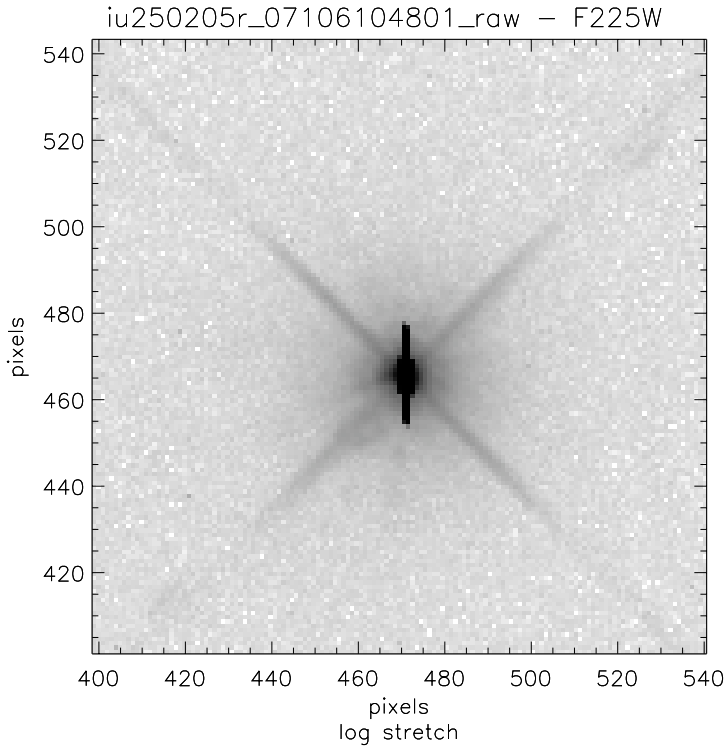

Figure 2: The same as in Figure 1, but for the F225W filter. A weak donut ghost (0.1%) is apparent to the lower left of the source. The plot here is zoomed out to show more of the diffraction spikes, because some flaring of the diffraction spikes in the upper right and lower left is noticeable, but these features are apparently due to a diffraction phenomenon unrelated to the filter (see Hartig 2004, ISR WFC3 2004-08). At other field points (see Figure 22), multiple donuts appear, with the total signal in all donuts at 0.4% the source signal.

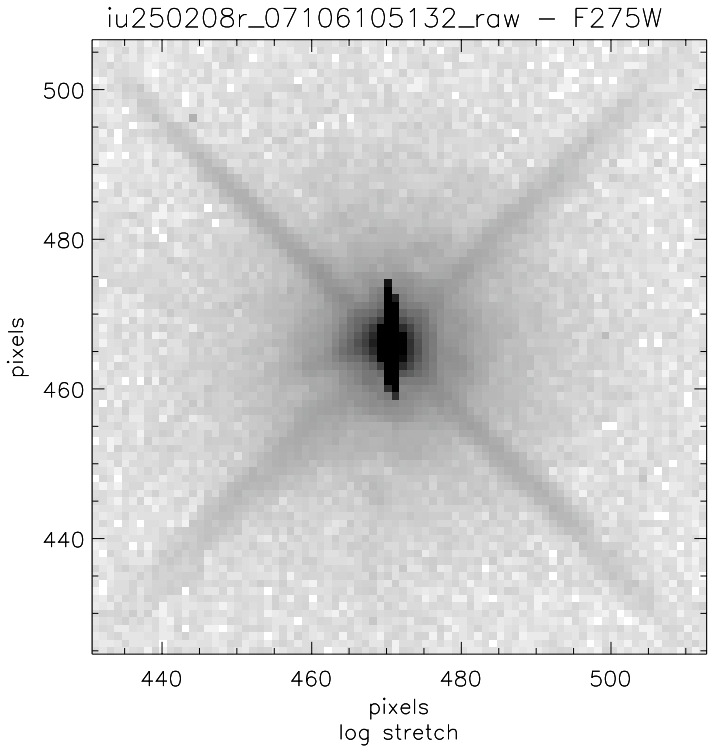

Figure 3: The same as in Figure 1, but for the F275W. No obvious ghosts are apparent. A small blip 20 pixels below the source contains much less than 0.1% of the source flux.

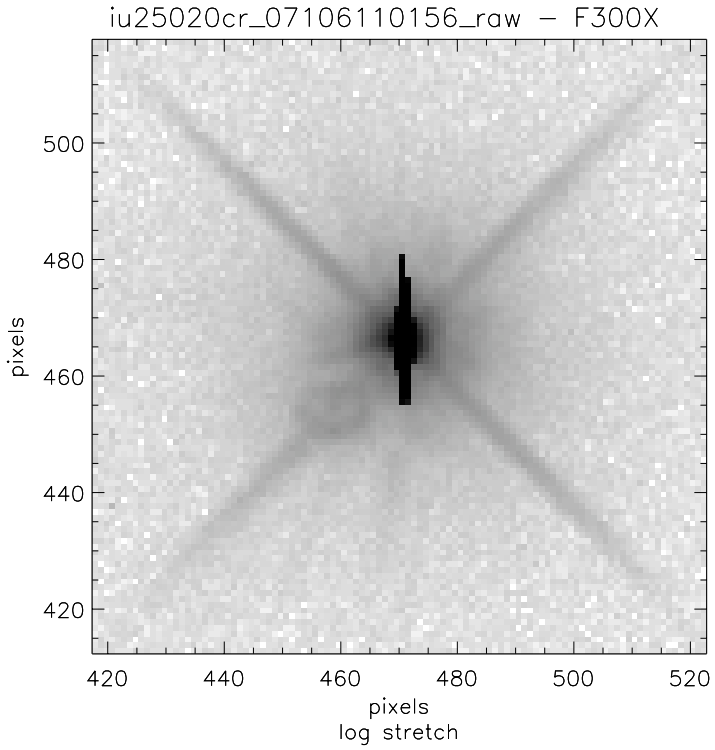

Figure 4: The same as in Figure 1, but for the F300X. A donut ghost (0.3%) is apparent to the lower left of the source.

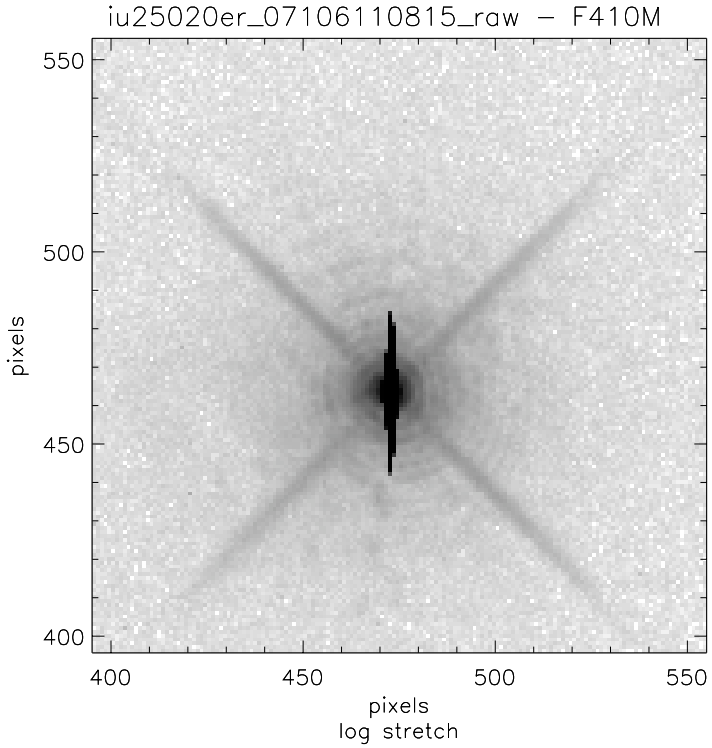

Figure 5: Same as in Figure 1, but for the F410M. Below the source, small compact artifacts are apparent that might be filter ghosts, but the total signal in these artifacts is less than 0.1% of the source signal.

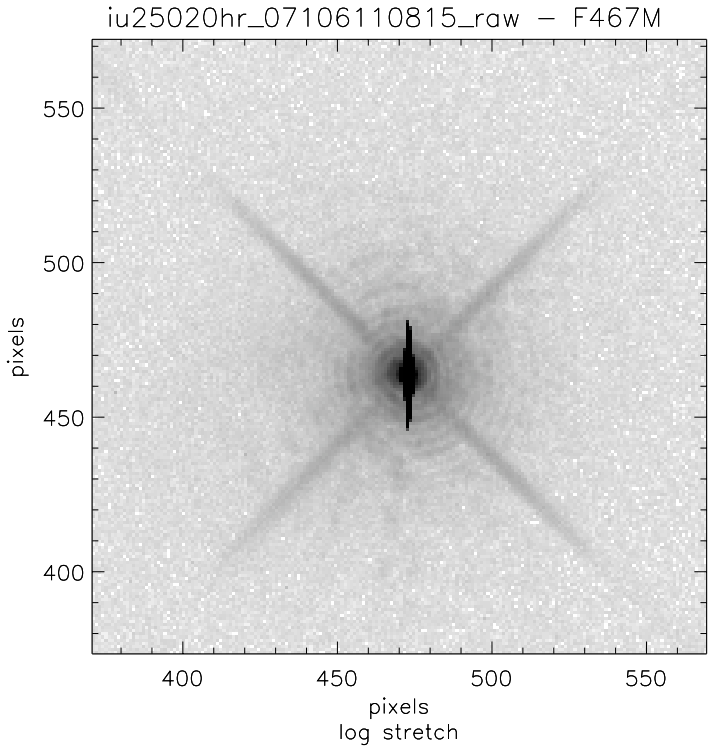

Figure 6: Same as in Figure 1, but for the F467M. Below the source, small compact artifacts are apparent that might be filter ghosts, but the total signal in these artifacts is less than 0.1% of the source signal.

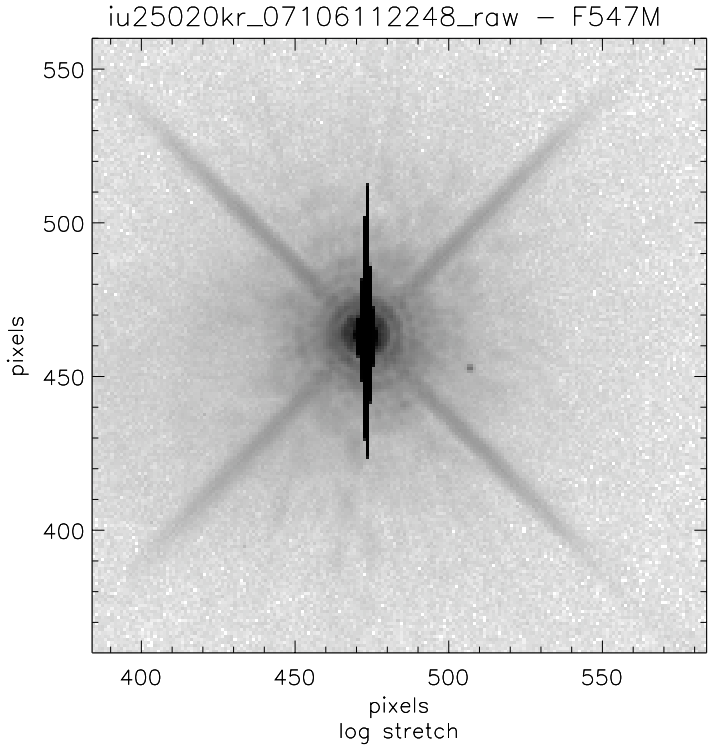

Figure 7: Same as in Figure 1, but for the F547M. This filter was not replaced. As in 2004, faint donut ghosts and compact ghosts are present, but the signal in these ghosts is less than 0.1%.

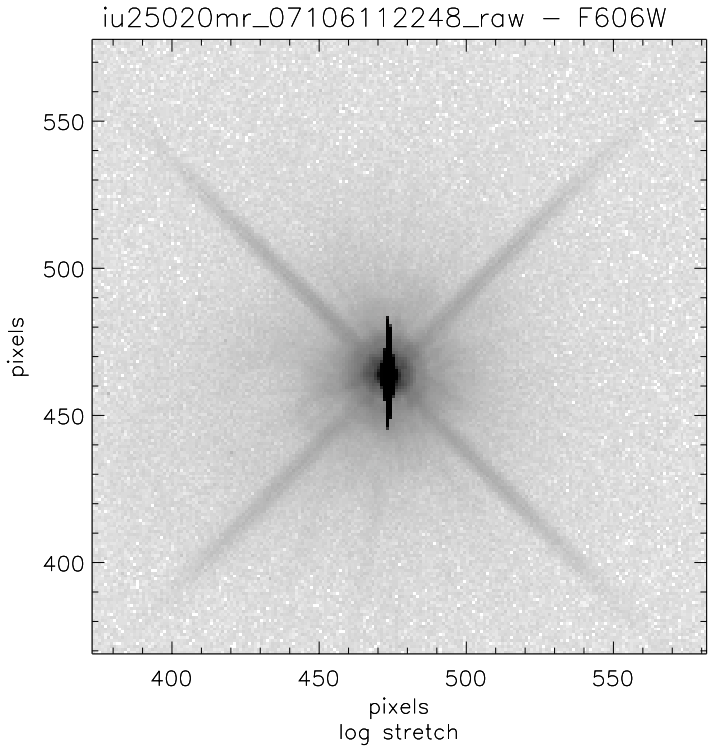

Figure 8: Same as in Figure 1, but for the F606W. Faint, extended donut ghosts can be seen to the lower left of the source, with the signal at 0.4% of the source signal. These donuts are due to the CCD windows, and were seen in the tests of the first F606W filter. Those tests also found many compact ghosts at the ~0.1% level, and those compact ghosts are no longer apparent in the images through the new F606W filter.

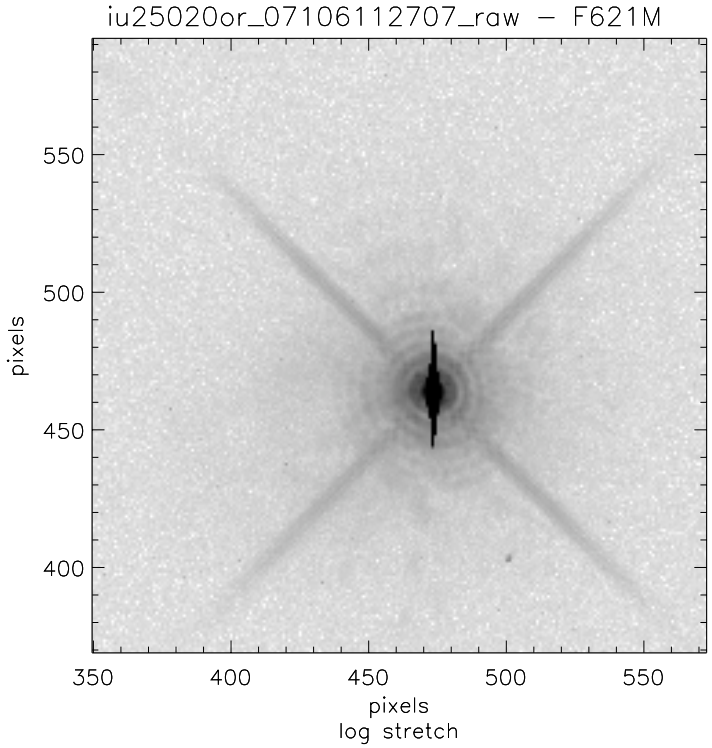

Figure 9: Same as in Figure 1, but for the F621M. Faint, extended donut ghosts can be seen to the lower left of the source, with the signal at ~0.2% of the source signal. These donuts are due to the CCD windows, and were seen in the tests of the first F621M filter. Those tests also found many compact ghosts at the ~0.1% level, and those compact ghosts are no longer apparent in the images through the new F621M filter. A faint spot about 50 pixels below the source appears to be a cosmic ray.

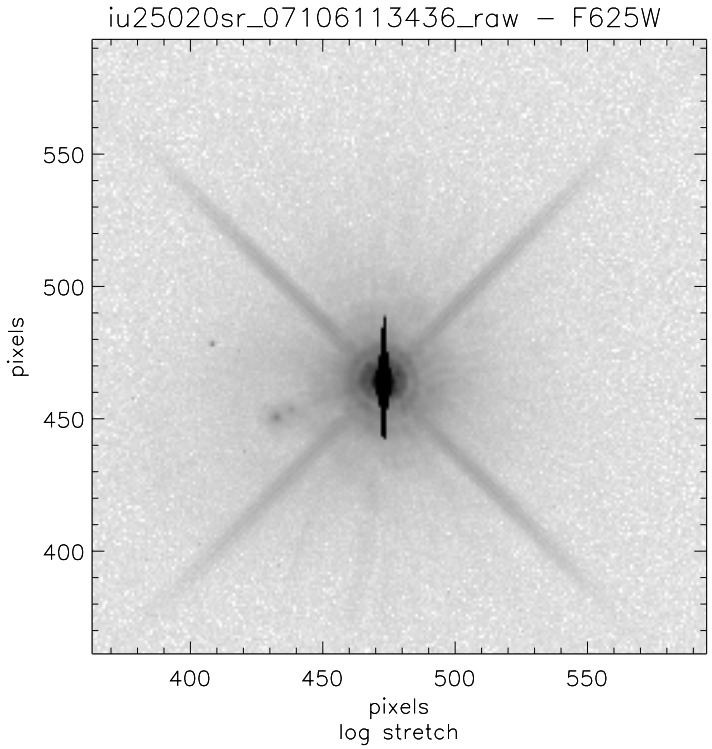

Figure 10: Same as in Figure 1, but for the F625W. This filter was not replaced. Faint compact ghosts and extended donuts can be seen to the left of the sources, with a total signal in all ghosts of 0.2% the source signal. Individual ghosts are <0.1%.

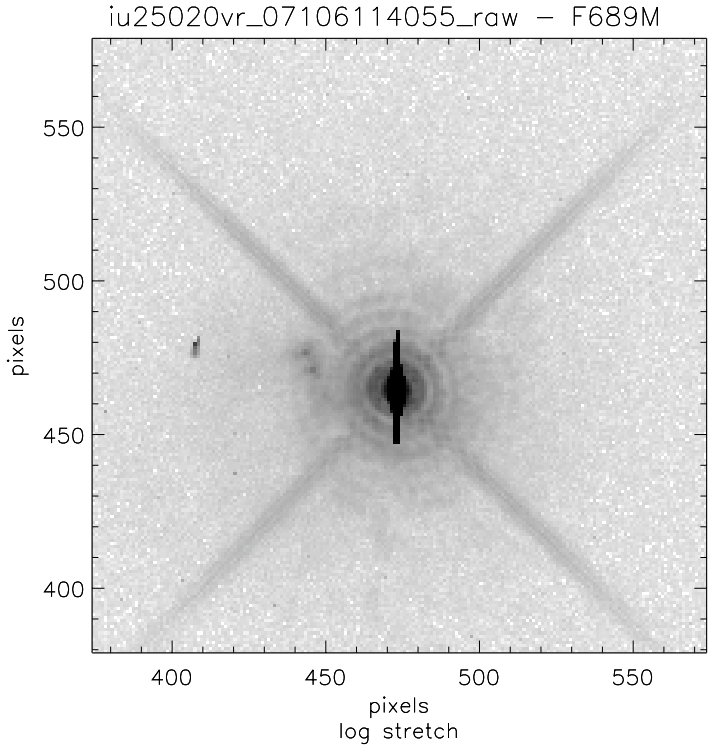

Figure 11: Same as in Figure 1, but for the F689M. This filter was not replaced. Compact ghosts and extended donuts can be seen to the left of the sources, with the total signal in all ghosts at 0.5% of the source signal. The two obvious compact ghosts are at 0.1% of the source signal.

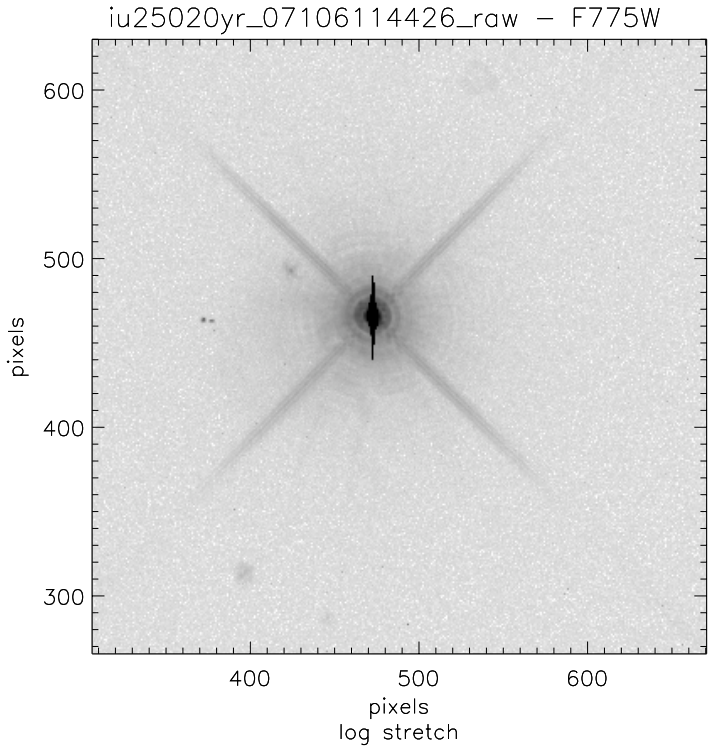

Figure 12: Same as in Figure 1, but for the F775W. This filter was not replaced. Compact ghosts and extended donuts can be seen in various directions, with the total signal in all ghosts at 0.3% of the source signal. Individual ghosts are at a signal < 0.1% of the source.

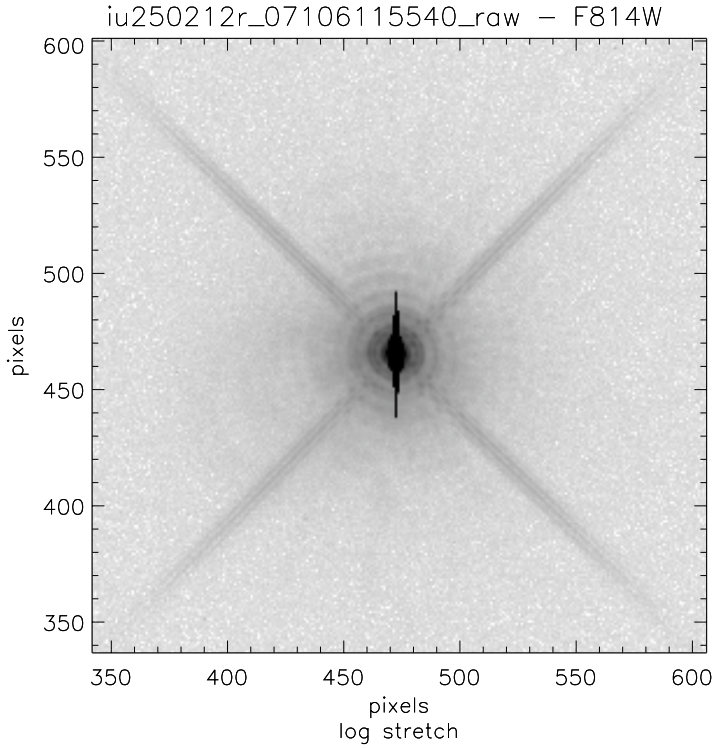

Figure 13: Same as in Figure 1, but for the F814W. This filter was not replaced. Two faint interlocking donut ghosts can be seen to the left of the source, while a smaller donut can be seen above the source. These donuts come from the CCD windows, and the total signal in these ghosts is 0.3% of the source signal.

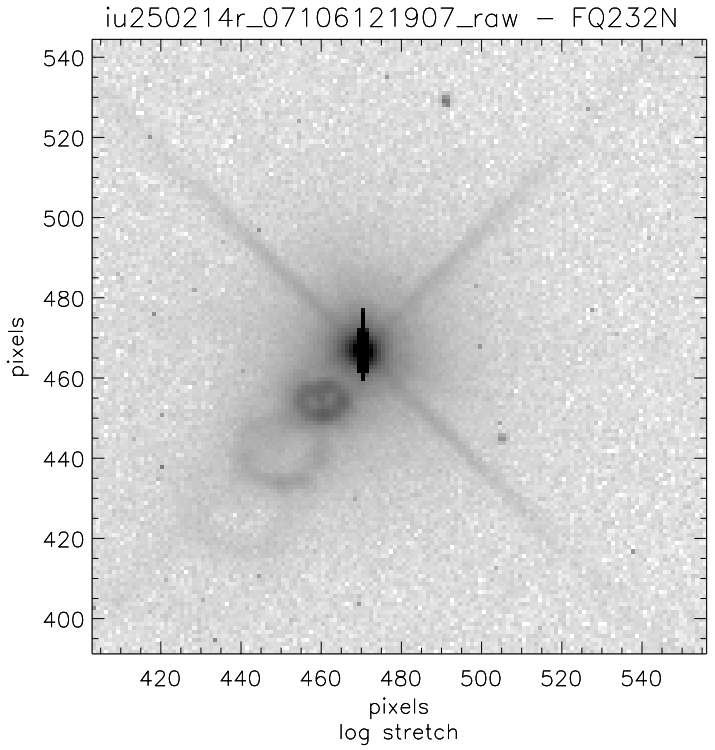

Figure 14: Same as in Figure 1, but for the FQ232N. This filter was not replaced. Three bright interlocking donut ghosts can be seen to the lower left of the source. The signal in the brightest ghost is 5% of the source signal, while the signal in all three ghosts is at 7% of the source signal.

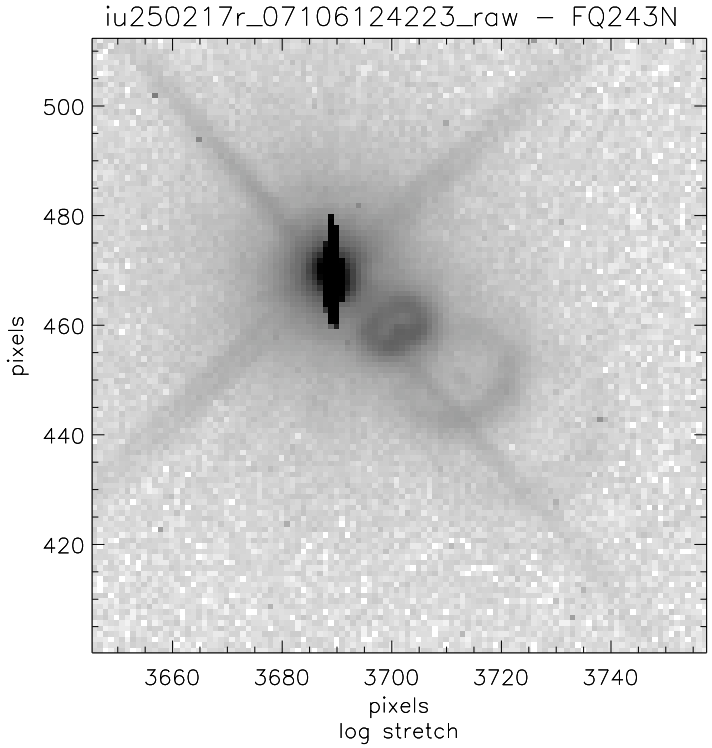

Figure 15: Same as in Figure 1, but for the FQ243N. This filter was not replaced. Three bright interlocking donut ghosts can be seen to the lower right of the source. The signal in the brightest ghost is 5% of the source signal, while the signal in all three ghosts is at 7% of the source signal.

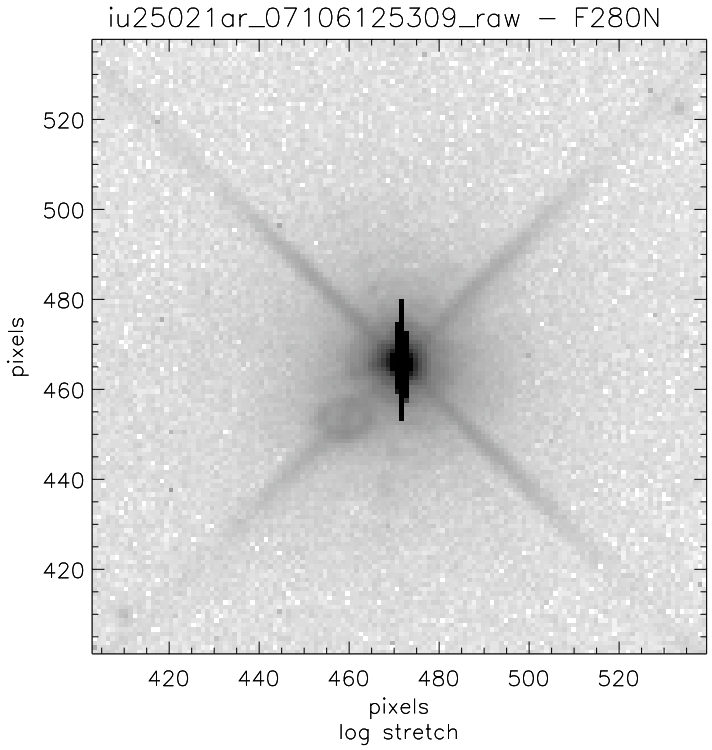

Figure 16: Same as in Figure 1, but for the F280N. A donut ghost can be seen to the lower left of the source, with the ghost signal at 0.3% of the source signal. When the source is placed at other field points (see Figure 23), the ghost strength is measured as high as 0.6%.

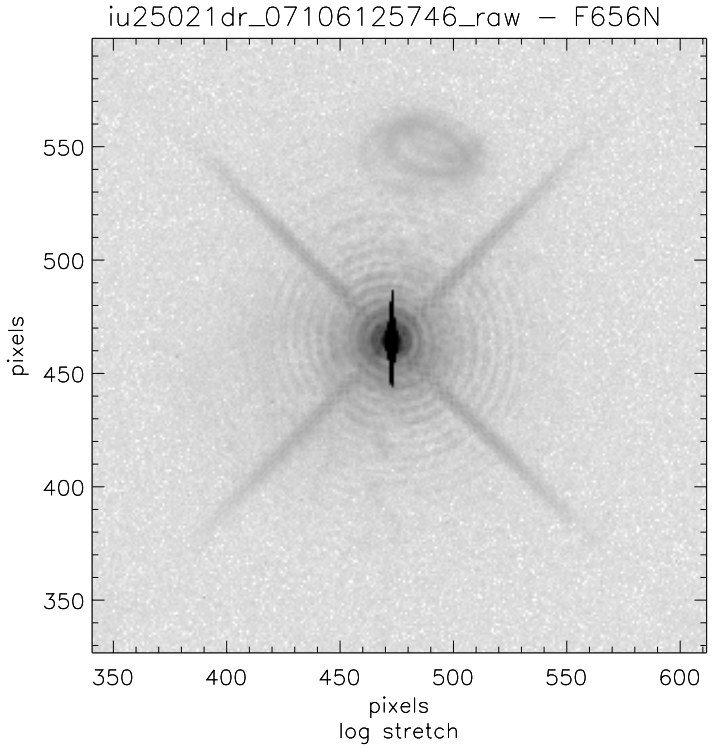

Figure 17: Same as in Figure 1, but for the F656N. This air-gap filter was not replaced. Interlocking filer ghosts appear above the source, with the total signal in those ghosts at 0.4% of the source signal. Faint window ghosts appear as donuts to the left of the source, but at less than 0.1% of the source signal.

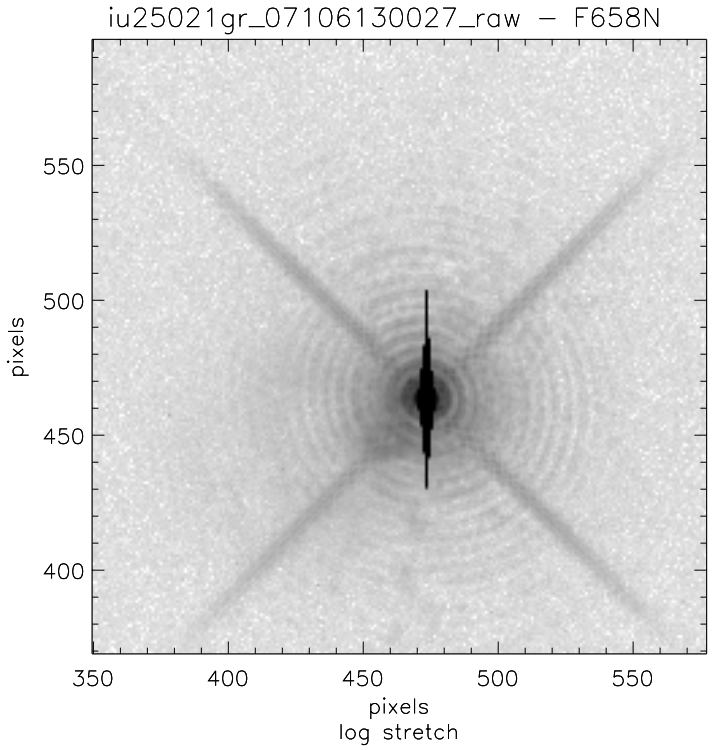

Figure 18: Same as in Figure 1, but for the F658N. A small donut-shaped filter ghost appears immediately to the lower left of the source, while faint extended donut ghosts from the window appear to the left of the source. The signal in the filter ghost is 0.4% of the source signal, while the signal in the window ghosts is 0.1% of the source signal.

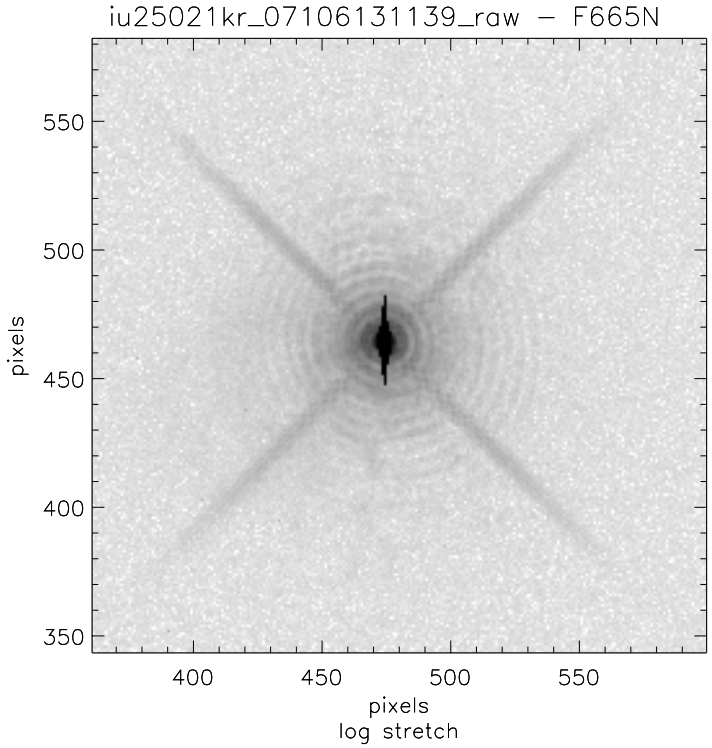

Figure 19: Same as in Figure 1, but for the F665N. This air-gap filter was not replaced. Faint extended donut ghosts from the window appear to the left of the source, while a more compact donut ghost from the filter appears to the lower left of the source. The window ghosts are at a strength of 0.2%, while the filter ghost is at a strength of 0.1%. This filter ghost looked stronger in 2004, although it is more difficult to characterize it at this field position, where it is closer to the point source.

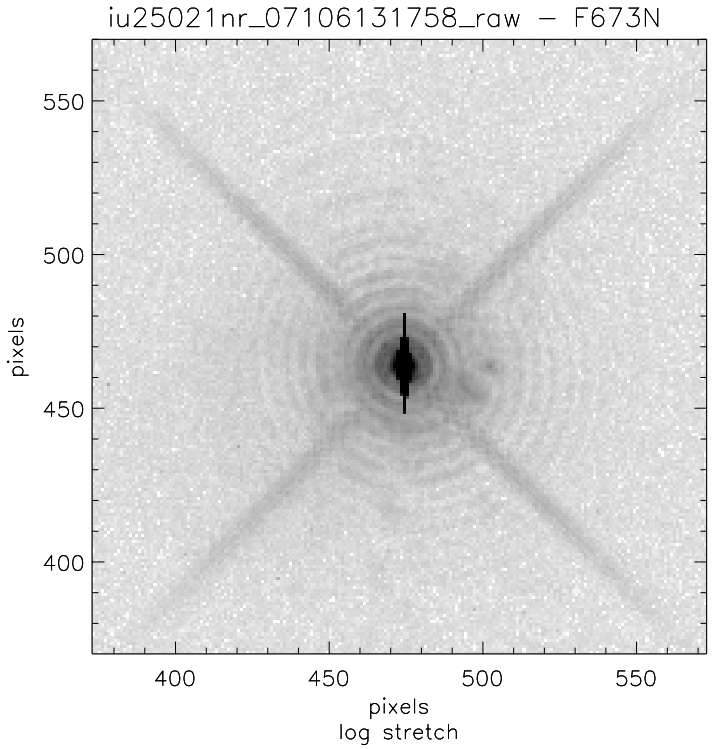

Figure 20: Same as in Figure 1, but for the F673N. This air-gap filter was not replaced. Faint extended window ghosts from the window can be seen to the left of the source, while more compact donut ghosts can be seen to the lower left of the source and also to the right of the source. The total signal in the filter ghosts is 0.3% of the source signal, while the signal in the window ghosts is 0.1% of the source signal.

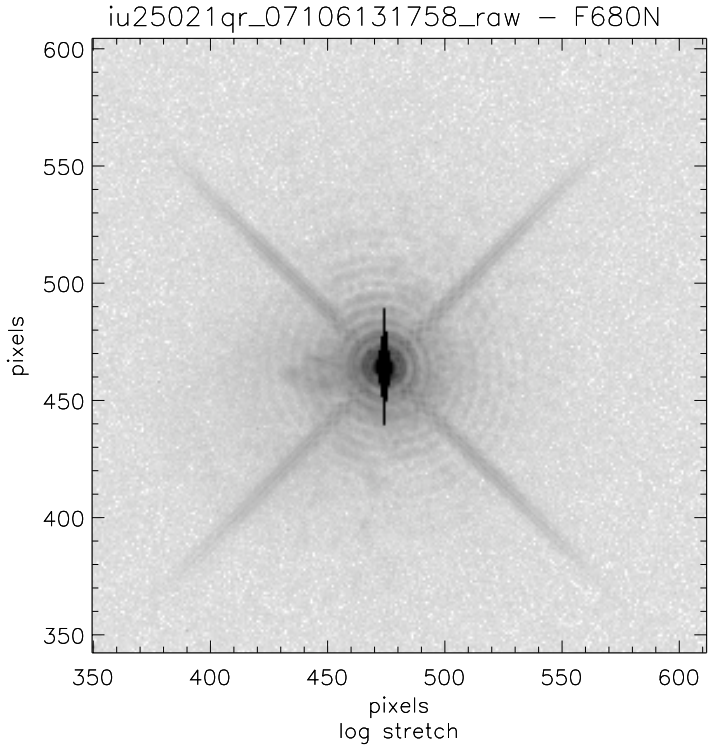

Figure 21: Same as in Figure 1, but for the F680N. This air-gap filter was not replaced. Faint extended window ghosts appear to the left of the source, while compact filter ghosts appear to the immediate left of the source. The window ghosts are at 0.1% of the source signal, while the filter ghosts are at 0.3% of the source signal.

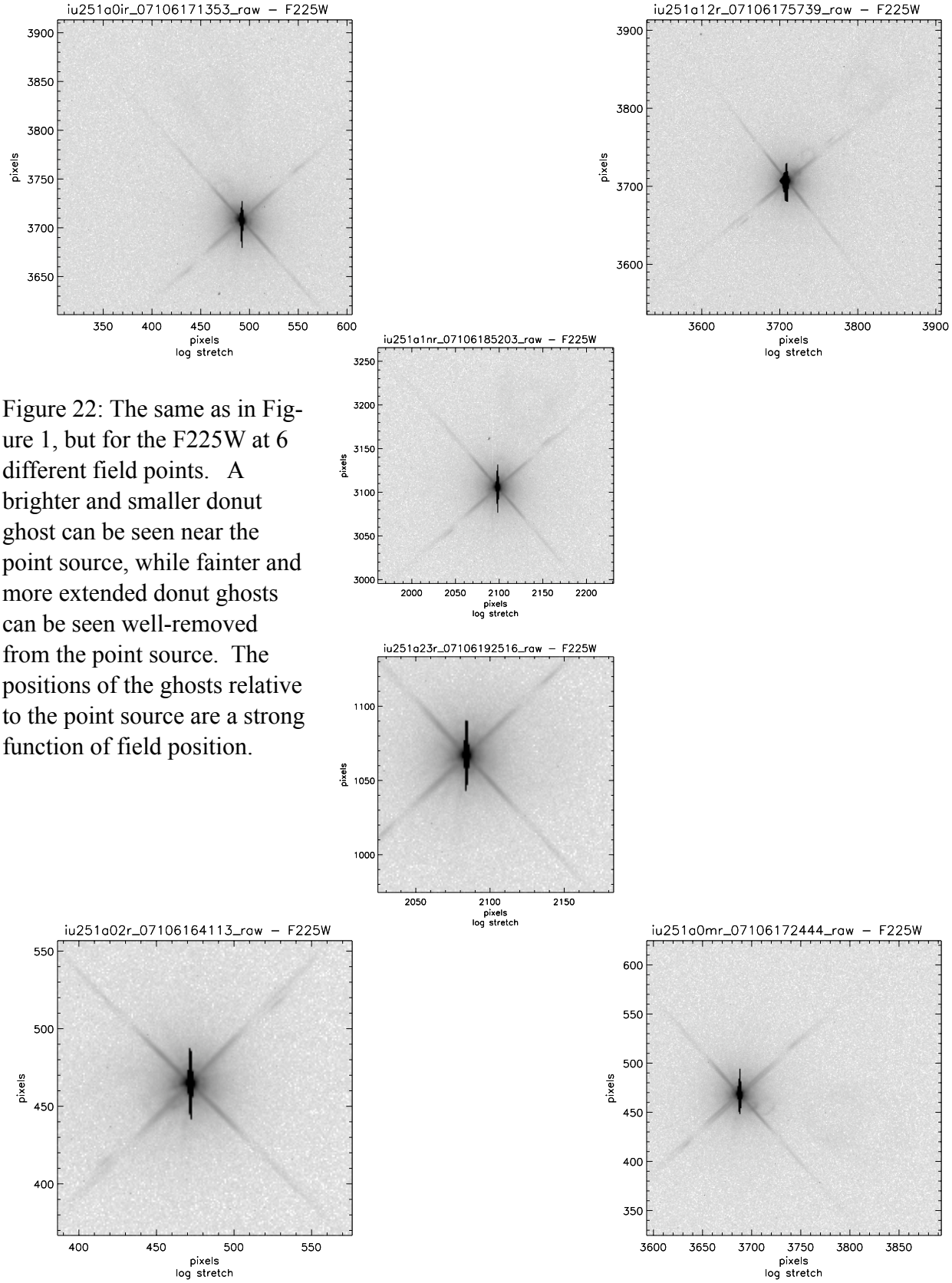

Figure 22: The same as in Figure 1, but for the F225W at 6 different field points. A brighter and smaller donut ghost can be seen near the point source, while fainter and more extended donut ghosts can be seen well-removed from the point source. The positions of the ghosts relative to the point source are a strong function of field position.

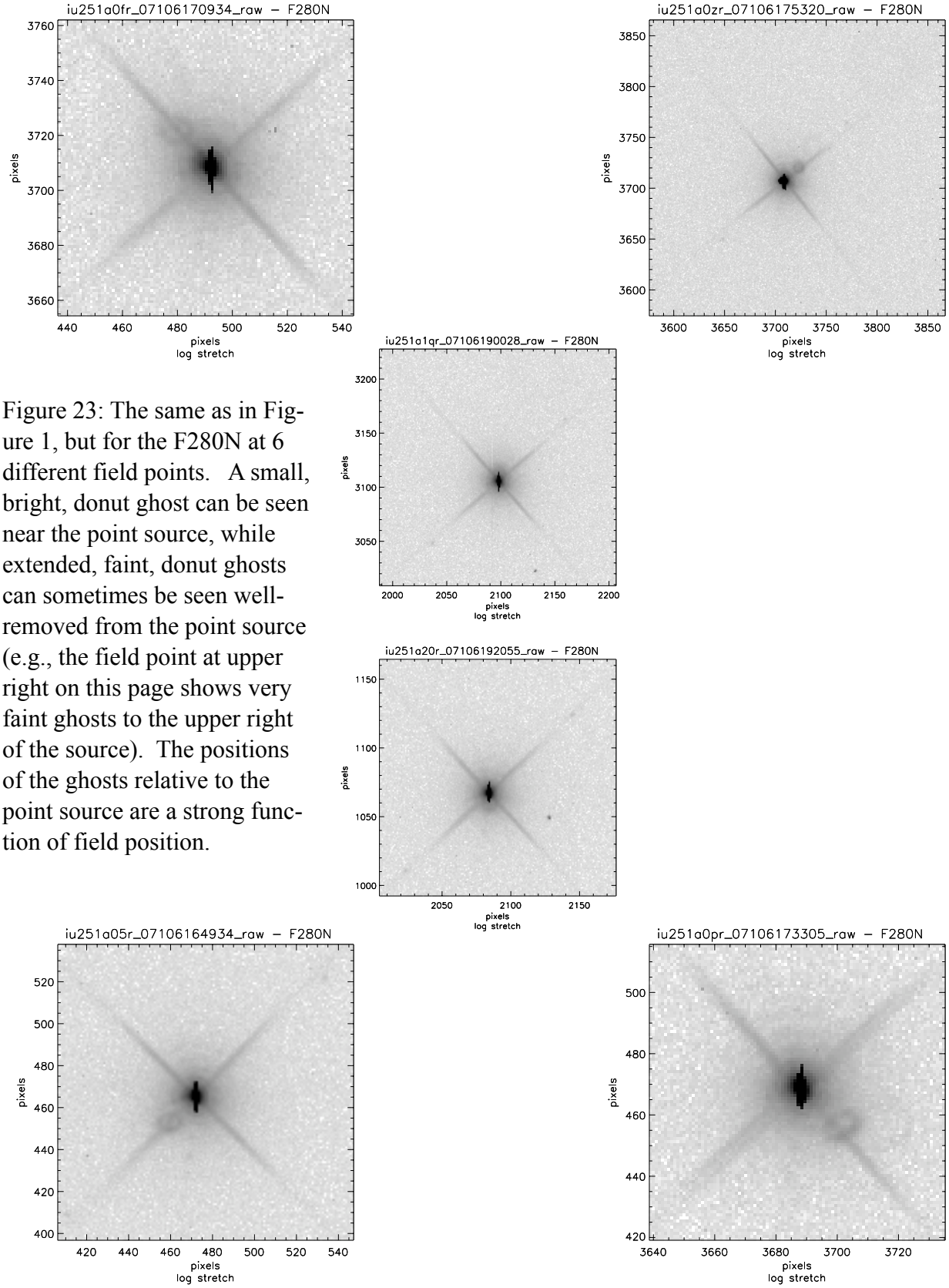

Figure 23: The same as in Figure 1, but for the F280N at 6 different field points. A small, bright, donut ghost can be seen near the point source, while extended, faint, donut ghosts can sometimes be seen well-removed from the point source (e.g., the field point at upper right on this page shows very faint ghosts to the upper right of the source). The positions of the ghosts relative to the point source are a strong function of field position.

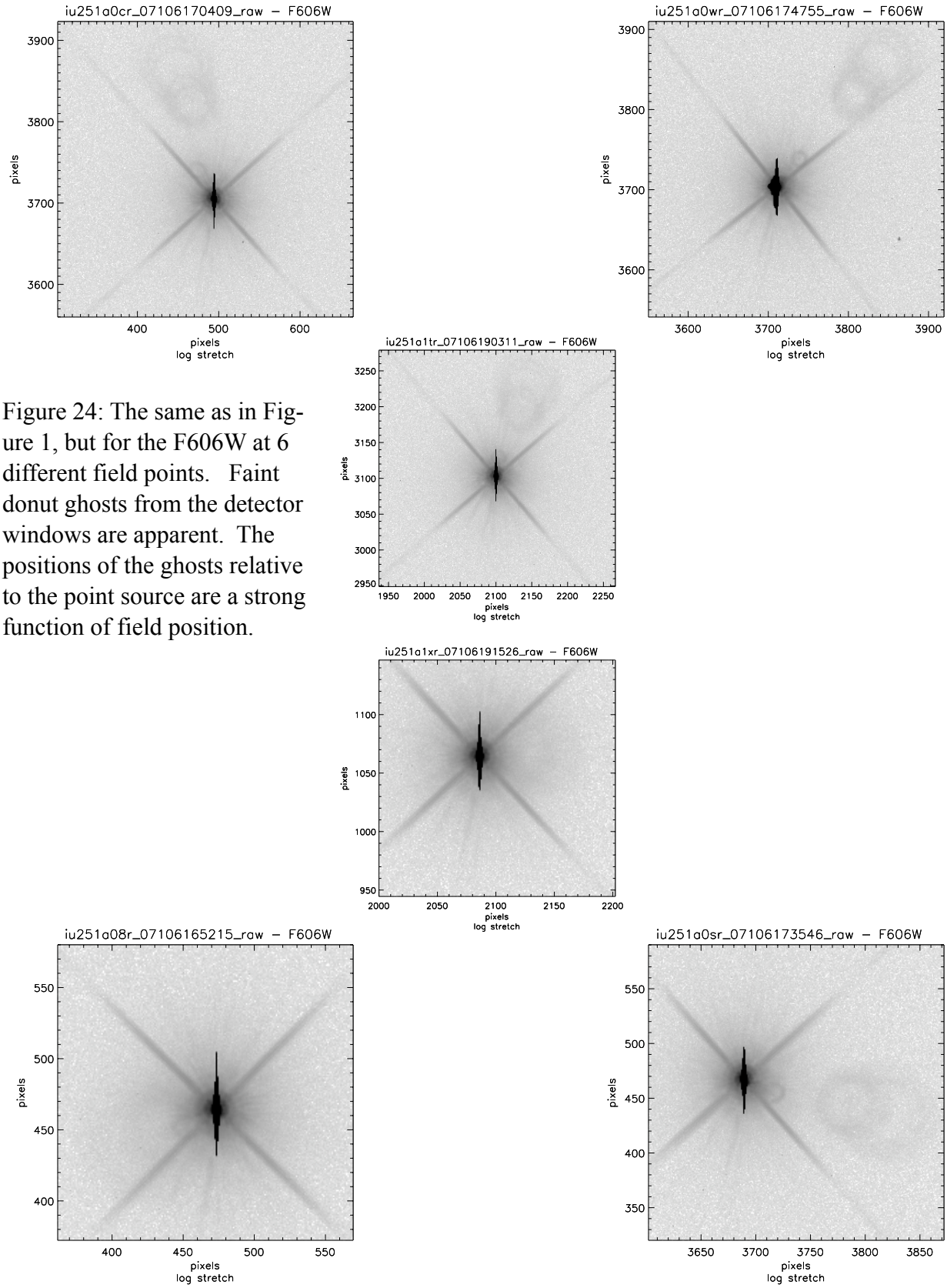

Figure 24: The same as in Figure 1, but for the F606W at 6 different field points. Faint donut ghosts from the detector windows are apparent. The positions of the ghosts relative to the point source are a strong function of field position.